Transcrystallinity Effects in High-Density Polyethylene. II. Determination of Kinetics Parameters

N. Billon, V. Henaff, J. M. Haudin

Centre de Mise en Forme des Matériaux, UMR CNRS 7635, Ecole des Mines de Paris, BP 207, 06904 Sophia-Antipolis Cedex, France

Received 9 May 2001; accepted 20 December 2001

ABSTRACT: Transcrystallinity may occur during differential scanning calorimetry analysis at the surfaces of the samples. In such a case, measurements may be unsuitable. We propose simple methods for the determination of intrinsic crystallization data that are accurate for the polymer and for the determination of the nucleating ability of the surfaces. These methods are based on the experimental analysis of the crystallization of samples with different and calibrated thicknesses during experiments at different constant cooling rates. Analysis of thin samples allowed the characterization of transcrystallinity, whereas analysis of at least three samples of different thicknesses allowed us to determine the true crystallization kinetics of the bulk material. These two techniques were independent of each other and were successfully applied to the case of a high-density polyethylene. The determinations were verified with simple analytical models. A further extension could be the study of the nucleating ability of different substrates. © 2002 Wiley Periodicals, Inc. J Appl Polym Sci 86: 734–742, 2002

Key words: crystallization; kinetics (polym.); transcrystallinity; polymer; spherulites; differential scanning calorimetry (DSC); high-density polyethylene (HDPE)

INTRODUCTION

During differential scanning calorimetry (DSC) analysis of polymers [e.g., high-density polyethylene (HDPE)], large transcrystalline regions may appear[1–3] at the contact between the material and the pans. This phenomenon, whose exact origin is not yet clearly established in the literature,[4] seems to result from an important nucleating ability of the surfaces, which promotes numerous additional spherulites.[5–11] Transcrystallinity is not a phenomenon specifically related to DSC analysis, but in this context, it represents a strong disturbing process. Some of its particular effects have been discussed in previous articles.[3,12,13] The crystallization traces and, accordingly, any data deduced from them depend on the cooling rate, the surface nucleation, the bulk nucleation, and the thickness of the sample. A theoretical model was developed[12] and applied to this technique to explain some experimental observations.[12,13] Unfortunately, this model, when expressed in its most general form, remains difficult to use for the interpretation of experimental results and for the extraction of intrinsic characteristics of the polymer.

The first part of this work was devoted to an experimental study of the crystallization of a HDPE that exhibited important transcrystallinity effects.[3] Experimental results were in agreement with our expectations, and the apparent behavior of this polymer was significantly modified by transcrystallinity. Relationships between DSC traces and transcrystallinity were sufficiently established to authorize further treatments of the results to deduce pertinent intrinsic data for the characterization of the crystallization of the polymer.

The aim of this second article is to propose simple models and simple experimental procedures to deduce accurate data for surface nucleation, on the one hand, and for bulk nucleation, on the other. This was done with crystallization at constant cooling rates, which was performed on samples having different calibrated thicknesses. Thin samples gave access to the characterization of surface nucleation, namely, the number of nuclei and the growth rate. Thicker samples enabled us to extract kinetics parameters for bulk crystallization. In the last part of the study, to validate the approach, we reproduced experimental DSC traces using simple models and the values of the parameters deduced from our analysis.

EXPERIMENTAL

The experiments were conducted with a HDPE grade (Eraclear IC 940 M) supplied by Enichem Polymres France, whose main characteristics were (1) average molecular weights: number-average (M_n) = 10,800, weight-average (M_w) = 39,000, and z-average (M_z) = 98,400 and (2) density = 0.9574 g/cm^3.

Disk-shaped specimens (diameter-6 mm) were cut from films of calibrated thicknesses (192, 315, 510, 651,

Correspondence to: N. Billon (noelle.billon@cemef.cma.fr).

Journal of Applied Polymer Science, Vol. 86, 734–742 (2002)

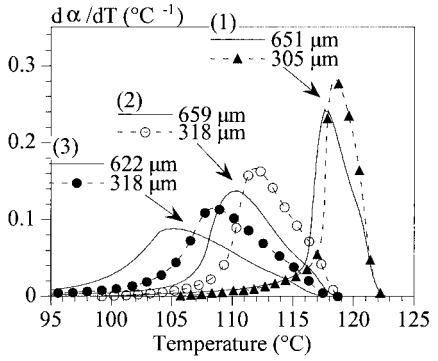

Figure 1 Experimental crystallization of approximately 315 and 651 μm thick samples. Evolution of $d\alpha/dT$ versus temperature for three cooling rates: (1) 1°C/min and 305 and 651 μm, (2) 10°C/min and 318 and 659 μm, and (3) 20°C/min and 318 and 622 μm.

and 865 μm on average)[3] and introduced into aluminum DSC pans. To obtain the films, we melted the pellets for 5 min at 180°C between two glass slides on a Mettler FP 52 hot stage and crystallized them in air. The DSC samples were rapidly melted in a PerkinElmer DSC-7, held for 5 min at 180°C, and then crystallized under constant cooling rates (ranging from 0.3 to 50°C/min). Integration of DSC traces gave access to the volume transformed fraction (α) and its rate ($d\alpha/dT$) as a function of temperature (T). We cautiously calibrated DSC apparatus to account for thermal resistance at different cooling rates.[3]

The experiments were discussed in the previous article.[3] Let us recall some of the main results. The DSC traces exhibited a complex shape. A shoulder existed at high temperatures. The shape of the peak and the location of its maximum in the temperature scale depended on both the cooling rate and the thickness of the sample (Fig. 1). Important transcrystalline regions existed on both sides of all the samples (Fig. 2). The amount of transcrystalline zones in the sample

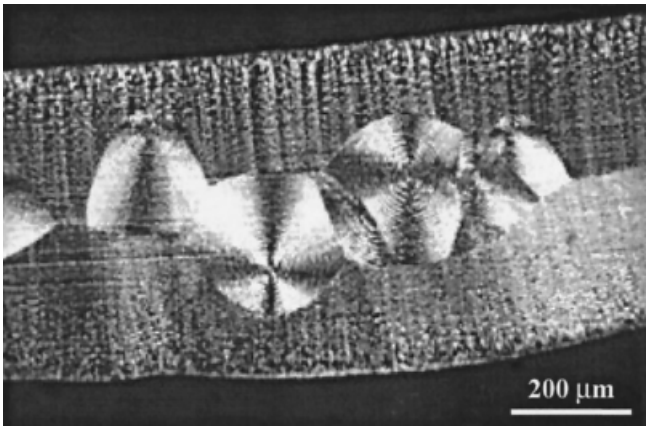

Figure 2 Crystalline morphology observed in a DSC sample with initial thickness of 650 μm after crystallization at a constant cooling rate.

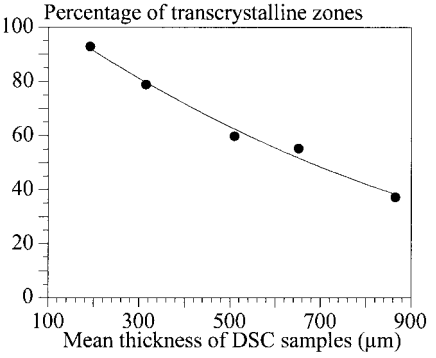

Figure 3 Amount of transcrystalline zone versus thickness of the sample.

was very important (Fig. 3). It ranged from 93% in the 192 μm thick sample and remained larger than 37% in the 865 μm thick specimens.

All the data were collected with a microcomputer, which ensured precise and easy manipulations and calculations. Due to transcrystallinity, these experimental data could not be manipulated in the classical way. Consequently, new methods have to be built up. We propose two methods for the determination of the contribution of trancrystallinity and bulk crystallization. These two methods are independent from each other and may be used separately.

Determination of intrinsic data

Growth rate

Transcrystallinity can be described as a two-step phenomenon: a nucleation phase, which can be described in a way similar to bulk nucleation,[7–10] and a growth phase. The growth phase is characterized by the growth rate of transcrystalline spherulites (G), which can reasonably be assumed to be equal to that of bulk spherulites (spherulites exhibit the same crystalline phase and the same ringed aspect).

According to previous analyses,[12,13] the shoulder is caused by a change in the growth geometry of the transcrystalline zones themselves: the morphology, initially consisting of semispherical spherulites, becomes continuous quasiplanar growth fronts. At this moment, semispherulites impinge on each other, and the transcrystalline zones become blocks with a quasiplanar surface. In parallel, the shoulder appears on the DSC traces, and α progressively becomes equal to

$$\alpha(t) = \frac{2}{e}\left[\int_0^t G(u)du\right] \quad (1)$$

where t, T, α, and e are the time, the temperature, the transformed volume fraction, and the thickness of the sample, respectively. As the cooling rate (T_p) is con-

stant during the crystallization, it is possible to relate the temperature to the time, and eq. (1) can be rewritten:

$$\begin{cases} \alpha(t) = \dfrac{2}{eT_p}\Re(T) \\ \Re(T) = \displaystyle\int_{T(0)}^{T(t)} G(\Gamma)d\Gamma \end{cases} \quad (2)$$

Then

$$T_p e \frac{d\alpha[T(t)]}{dT} = 2G[T(t)] \quad (3)$$

According to microscopic observations, 192 μm thick samples are roughly entirely transformed by transcrytsalline entities.[3] So, the DSC traces associated with them are mainly representative of the kinetics of transcrystalline crystallization.

Within the frame of the previous assumptions, experimental α values should obey eq. (2) at sufficiently high αs. From an experimental point of view, this dependence on cooling rate (α proportional to $1/T_p$) was observed for αs ranging from 15 to 30%. At a higher conversion ratio, contributions of volume nucleation and possibly of the secondary crystallization were less negligible. Experimental values for the parameter $T_p e d\alpha/dT$ are plotted versus temperature for 18 different cooling rates in Figure 4. Despite a certain scattering, the values were roughly organized in a master curve. According to eq. (3), this curve should represent G. With a mean-squares method, it is possible to fit this data to estimate G. For convenience, we chose a simple expression, already used in the past at low supercooling for polyethylene:[1,14–17]

$$G(T) = G_o \exp\left[-\frac{A}{T(C-T)}\right] \quad (4)$$

where G_o, A, and C are constants. The best agreement (Fig. 4, curve 2) would be obtained for

$$\begin{cases} G_o = 288.1\ \mu\text{m/s} \\ A = 28202\ \text{K}^2 \\ C = 404\ \text{K} \end{cases} \quad (5)$$

These numerical values are of the same order of magnitude as data reported in the literature,[1] that is, G_o ranging from 300 to 1100 μm/s, A ranging from 7×10^4 to 9×10^4 K^2, and C equal to 418 K. However, from a theoretical point of view, C in eq. (4) should represent the equilibrium melting temperature (T_{om}).[15–17] The obtained value of 131°C seemed far too low for HDPE, especially if one considers that the melting temperature of this polymer (determined by DSC at a heating rate of 10°C/min) varied from 134 to 126°C,[18] depending on the cooling rate, which ranged from 0.1 to 50°C/min. Consequently, such a C value could not be accepted from a physical point of view. If a more realistic value was imposed (i.e., 418 K, i.e., 145°C), it was also possible to fit the experimental data in Figure 4. For example, if C is equal to 418 K and G_o is equal to 25,000 μm/s, curves 1 and 4, corresponding to A = 112,000 and 103,000 K^2, are bounds of the experimental variations of G. Additionally, an average value of 106,000 (Fig. 4, curve 3) leads to an agreement equivalent to the previous one. Consequently, such a determination for G is rather imprecise, and the results should be regarded only as estimates.

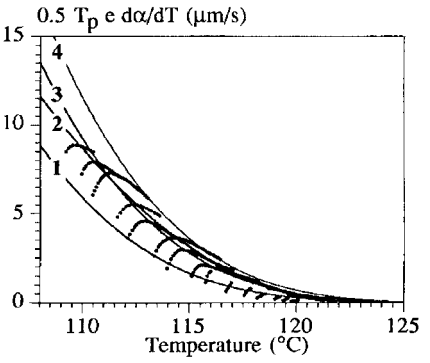

Figure 4 Experimental evolution of $0.5T_p e\, d\alpha/dT$ as a function of the temperature (α = 15–30%). Comparison between (·) experimental value and (—) calculation according to different estimates for G. (1) T_{om} = 418 K, G_o = 25,000 μm/s, A = 112,000 K^2; (2) T_{om} = 404 K, G_o = 288.1 μm/s, A = 28,202 K^2; (3) T_{om} = 418 K, G_o = 25,000 μm/s, A = 106,000 K^2; and (4) T_{om} = 418 K, G_o = 25,000 μm/s, A = 103,000 K^2.

It would be interesting to confirm these data, for example, using crystallization on a hot stage between glass slides. Unfortunately, this polymer also developed an important transcrystalline region at the contact with the glass. It was impossible to avoid it, even when we used molding agent to treat the glass surfaces. As a consequence, optical measurements for G were impossible. The determination of T_{om} with DSC determination of melting temperature as a function of crystallization temperature was also impossible because of transcrystallinity. To partly overcome these limitations, we compared estimates using eq. (4) and the two best sets of parameters determined previously to some experimental data reported in the literature (Fig. 5). These latter were obtained:

- Above 120°C with optical microscopy and a commercial HDPE[19] (M_n = 26,000, M_w = 160,000) and a fraction of average weight mass equivalent to ours (35,000).[20,21]
- At low temperature[22] with a commercial HDPE of density 0.965 and an astute method based on the measurement of the thickness of the transcrystal-

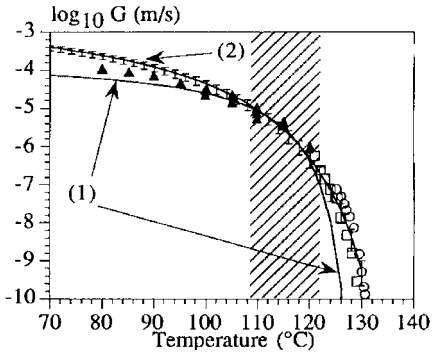

Figure 5 Evolution of log G as a function of temperature. Comparison between experimental data from the literature: (□) ref. [19], (○) refs. [20] and [21], (▲) ref. [22], and (—) our estimates. (1) eqs. (4) and (5) and (2) A = 106,000 K^2, G_o = 25,000 μm/s, C = 418 K (error bars correspond to values for A = 112,000 and 103,000 K^2).

line zone induced at the contact with a quenched surface.

In Figure 5, the hatched region represents the range of temperature in which G was estimated in this work. The two sets were in good agreement with experimental values from the literature in that range. Moreover, extrapolations towards either higher or lower temperatures were also in pretty good agreement with reported experimental data, especially when the second set was used (A = 106,000 K^2, G_o = 25,000 μm/s, C = 418 K, Fig. 5, curve 2).

In spite of the lack of precision, it must be emphasized that the only parameter to be considered was $\Re(T)$; a precise determination for each of the parameters of eq. (4) was not necessary. A good mathematical fit for G was sufficient.

Nucleation rate

Coming back to low αs (0.1–10%), we were able to characterize surface nucleation. Optical observations showed that the nucleation process was more efficient at the surface than in the volume; if not, the transcrystalline zones would not be so large (compared to the maximum size of core spherulites) and so continuous that core spherulites should disturb their growth. In addition, the boundaries between transcrystalline spherulites were straight lines. This implied that their nucleations were almost simultaneous; if not, these boundaries should be hyperbolic lines. Hence, an instantaneous nucleation was first assumed.[12,13] In such a case, the very first steps of the transformation could be described as a function of time with a simple equation:

$$\alpha(t) = \frac{4\pi N_s}{3e}\left[\int_0^t G(u)du\right]^3 = \frac{4\pi N_s}{3e}\left[\frac{\Re(T)}{T_p}\right]^3 \qquad (6)$$

where N_s is the number of nuclei per unit surface. In fact, a more general expression for α could be established (see Appendix), and this equation has to be regarded as an approximation. If the first set of estimated parameters is used in the expression of G (C = 404 K), eq. (6) is verified, as shown in curve 1 of Figure 6. The 18 experimental cooling rates led to a master curve $\ln(\alpha e) + 3\ln|T_p|$ vs. $\ln|\Re(T)|$, whose slope was 3.09 and whose ordinate was −6.09. In such a case, the transcrystalline crystallization could be described by the instantaneous nucleation of 5×10^{-4} [$N_s = (3/4\pi)\exp(-6.09)$] spherulites/$\mu$m^2. This value was rather close to that given in the case of polyamide 6-6 ($N_s = 2 \times 10^{-3}$ μm^{-2}).[12]

If estimates based on the more accurate value C = 418 K were used for G, it was impossible to draw an equivalent master curve. Therefore, it was inferred that nucleation might be sporadic in time. We then assumed a constant nucleation rate per unit surface (ν). Within the frame of the isokinetic assumption, often used in the field of polymers (G/ν constant)

$$\nu = \nu_0 \frac{G}{G_0} \qquad (7)$$

where ν_0 is a constant. Then

$$\alpha(t) = \frac{\pi}{3}\frac{\nu_0}{eG_0}\left[\frac{\Re(T)}{T_p}\right]^4 \qquad (8)$$

As a consequence, $\ln(\alpha e) + 4\ln|T_p|$ should have linearly depended on $\ln|\Re(T)|$ with a slope equal to 4. The experimental results, interpreted with the average and extreme values for A in eq. (4), were roughly organized into a master curve. The best agreement was observed for the average value (Fig. 6, curve 2), with a

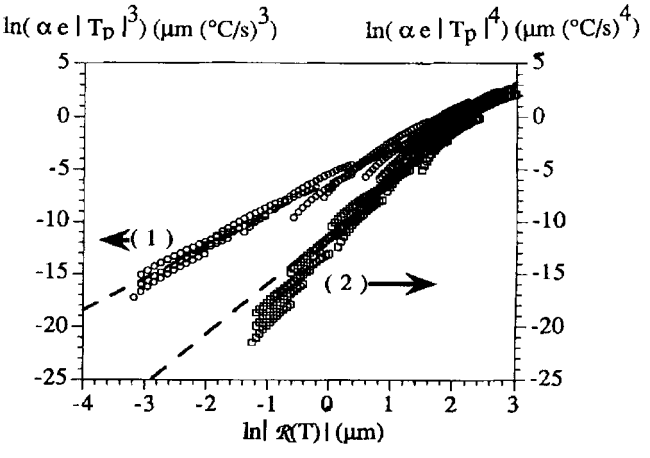

Figure 6 Experimental estimates for surface nucleation parameters as a function of temperature: (1) instantaneous assumption with G = 288.1exp[−28,202/T(404−T]-μm/s and (2) sporadic assumption with G = 25,000exp[−106,000/T(418−T)]-μm/s.

TABLE I
Values of the Slope of the $\ln(\alpha e T_p^4)$ versus $\ln|\Re|$ Curve for Three Different Estimated Values of A

A (K^2)	Minimum	Maximum	Medium
103,000	4.4	8.1	5.7
106,000	3.5	6.1	4.7
112,000	4.1	7.6	5.3

mean slope equal to 4.7 (Table I) and a mean ordinate equal to −12. Despite the extreme sensitivity to G and the imprecision of its determination (concerning especially T_{0m}), we can conclude that surface nucleation should be close to a sporadic in time one with a parameter ν_0 equal to 0.04 $\mu m^{-2}\ s^{-1}$.

In conclusion, with this method, it is possible to partly characterize transcrystalline nucleation. The main problem remains the measurement of G, as DSC analysis does not seem to lead to precise estimate for G. A better determination would require complementary techniques. Nevertheless, we are able to model the average evolution of α related to transcrystallinity in two approximate ways, that is, an "equivalent instantaneous case" and a sporadic in time nucleation. From a physical point of view, the last solution seems more satisfactory, whereas the first one is simpler to use.

Characterization of bulk crystallization

It was suggested and demonstrated[12] that because of the difference of the geometric location of the nuclei, it is possible to decompose the transformed volume (V_{tran}), into two separated volumes: the volume overlapped by transcrystalline entities (V_{sur}) and the volume transformed by bulk spherulites (V_{vol}).

Consequently, at any time

$$V_{tran} = V_{sur} + V_{vol} \tag{9}$$

It is impossible to decompose the DSC traces into these two components. Let us call V_{tot} the total volume of the sample:

$$V_{tran} = \alpha V_{tot} \tag{10}$$

The bulk crystallization can be characterized by a bulk volume transformed fraction (α_v). α_v is fraction of the volume that would be transformed in the polymer in the case where there was absolutely no transcrystallinity. As bulk crystallization only concerns the volume that is not yet overlapped by transcrystalline zones, α_v is given by

$$\alpha_v = \frac{V_{vol}}{(V_{tot} - V_{sur})} \tag{11}$$

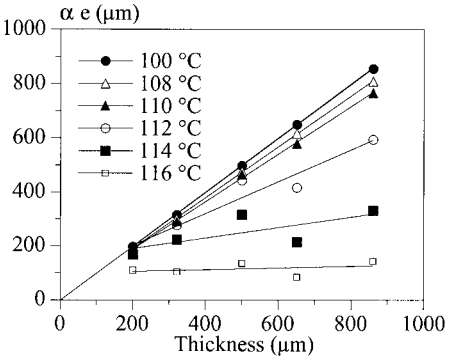

Figure 7 Determination of bulk crystallization. Evolution of αe versus sample thickness at different temperatures for a cooling rate of 5°C/min.

Equation (11) gives the intrinsic parameter able to characterize the crystallization kinetics in the polymer. Equations (9), (10), and (11) lead to

$$\alpha = \alpha_v + (1 - \alpha_v)\frac{d}{e} \tag{12}$$

where d is the total thickness of the transcrystalline zones (cumulated on both sides of the sample) and e is the thickness of the specimen. α_v and d only depend on the cooling rate and the temperature. So, when αe is plotted at a given cooling rate and temperature versus sample thickness, it should obey a linear variation whose slope is α_v and whose origin is $(1 - \alpha_v)d$. This was the case at low cooling rates (Fig. 7): at any temperature, a straight line was obtained whose slope increased from 0 to a maximum of 1 when the temperature decreased. At higher cooling rates (Fig. 8), a decrease of the slope was observed for high thicknesses. This should be related to thermal gradient within the sample. For this reason, thicknesses larger than 651 μm were ignored for the calculation of the slope.

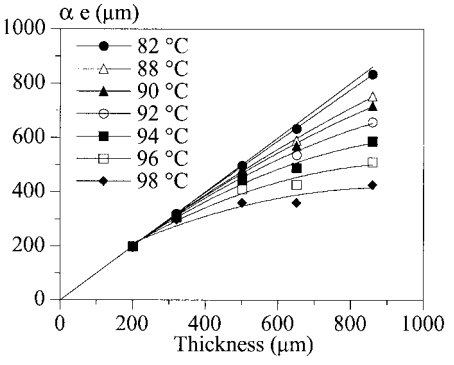

Figure 8 Determination of bulk crystallization. Evolution of αe versus sample thickness at different temperatures for a cooling rate of 50°C/min.

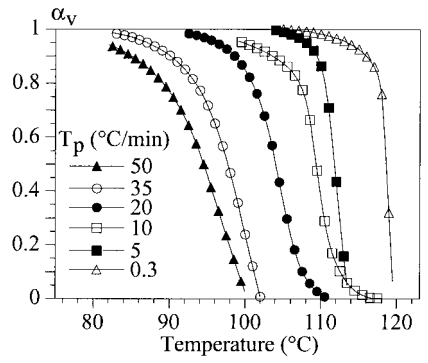

Figure 9 Evolution of bulk transformed volume fraction (α_v) versus temperature for different cooling rates (T_p's).

With this procedure, it was possible to determine α_v as a function of temperature and cooling rates ranging from 0.3 to 50°C/min (Fig. 9). This estimate seemed to be qualitatively correct because the general form of the transformation curves was reproduced and the usual effect of cooling rate was observed: the faster the cooling was, the lower the temperature of crystallization was. In addition, true crystallization temperatures for this HDPE could now be determined. For convenience, they were chosen at the maximum of the peak $d\alpha/dT$ versus T (Table II). These temperatures were very close to those measured with 865 μm thick samples, but were generally a little lower. They were also lower than the temperatures measured with thinner samples (192 μm, Table II), especially at high cooling rates. Normal samples (300–400 μm thick) led to a significant overestimate of the crystallization temperature because transcrystallinity was still relatively important in these cases. This overestimate would induce erroneous calculations if such data were used in a model for the simulation of crystallization during processing. It would be tempting to perform measurements on thick samples. Nevertheless, measurements on samples as thick as 865 μm may be dangerous, especially for high cooling rates (i.e., higher than 30°C/min) because of the thermal gradient that can be developed inside the polymer.

Conclusions

In conclusion, even if not totally satisfactory, the methods developed here appear to be more accurate solutions than the usual ones for the interpretation of the DSC curves. They make it possible to characterize the crystallization of a polymer with DSC analysis, even when transcrystallinity disturbs the measurements. Their main advantages are their simplicity and the fact that they do not require additional techniques (assuming G is known). One of the methods is dedicated to the characterization of transcrystallinity; the other one is dedicated to the characterization of the polymer itself.

Obviously, the latter of these proposals may seem tedious because it involves experiments at several cooling rates, several sample thickness (at least three), and mathematical manipulations to get plots as presented in Figures 7 and 8. However, because computers are now used extensively in experimental analysis, this does not represent an actual limitation.

The former of these methods allows a simple characterization of the nucleating ability of aluminum on the polymer. One could envision, provided that additional thermal resistance can be accounted for, using other materials for the DSC pans or testing sandwiches to characterize nucleating ability of another material (e.g., materials used as fibers in composites) in a quite innovative way.

Validation

Introduction

To validate these two methods, experimental DSC traces were reproduced with eq. (12) and data obtained in the previous section. To achieve this, it was first necessary to fit α_v and V_{sur} with accurate mathematical expressions. We needed the estimate of nucleation parameters for the bulk polymer to use a rigorous model (e.g., those developed in previous articles[12,23,24]). So, for convenience, and simplicity, we chose an Ozawa dependence[25] for α_v:

$$\alpha_v = 1 - \exp\left[-\frac{\chi(T)}{|T_p|^n}\right] \tag{13}$$

TABLE II
Comparison Between Crystallization Temperatures of the Polymer (Determined with Our Method) and the Apparent Crystallization Temperatures (Measured at the Maximum of the Peak) Determined by DSC with 865 and 192 μm Thick Samples

Cooling Rate (°C/min)	Crystallization Temperature (°C)		
	In the Volume	865 μm Thick Sample	192 μm Thick Sample
0.3	119	119.4	120.8
0.5	118	118.5	120
0.7	119	118.0	119.9
1	117	117.7	119.1
2.5	115	115.2	117.5
3.7	114	113.9	116.4
5	112	112.9	115.7
7.5	110	111.7	114.8
10	109	110.1	114.4
15	108	107.9	113
20	104	106.6	112.5
25	105	103.5	111.3
30	102	102.6	110.6
35	100	102.5	109.7
40	99	102.7	109.4
45	100	102.2	108.3
50	97	97.6	108.2

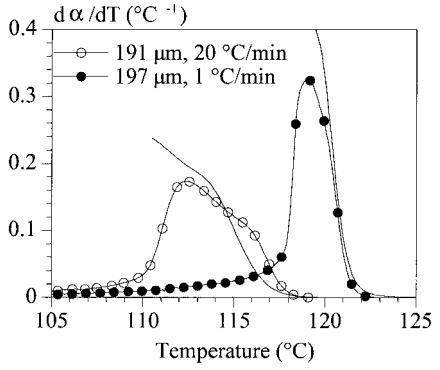

Figure 10 Comparison between (symbols) experimental DSC traces obtained with 192 μm thick samples and (—) calculations using eqs. (12–15).

where T_p is the cooling rate, n is the so-called Avrami-exponent, and χ is a function depending on temperature. A good agreement was found, between 116 and 120°C for $n = 2.2$, $\chi(T) = \exp(-155.25 + 3.2803T - 0.017385T^2)$, where T was in degrees Celsius. These parameters and eq. (13) made it possible to reproduce α_v for cooling rates lower than 20°C/min. Higher cooling rates would need a different expression for χ. Once again, we only aimed at fitting the experimental curves. The physical meaning of these values is out of the scope of this article and is not discussed.

With regard to V_{sur}, rigorous models have been developed[12,23,24] on the basis on Evans' approach[26] that enable us to predict the crystallization of a thin film of polymer. One of these models, combined with computer simulations and applied to the particular case of DSC analysis,[12,13] makes it possible to reproduce and understand crystallization traces as well as morphology development. These models are sometimes difficult to use because they involve parameters that are difficult to measure, especially the activation frequency. Consequently, to keep the simplicity to the approach, a simplified model was used (see Appendix). With the assumption of an instantaneous nucleation of numerous nuclei (whose number per unit surface is N_s) on both sides of the sample, the volume of the transcrystalline zones at any time t was written as

$$\frac{d}{e} = \frac{2R}{e} - \frac{2}{e}[\exp(-N_s\pi R^2)\int_0^R \exp(N_s\pi x^2)dx] \quad (14)$$

x defines the location inside the film (see Fig. A.1) and

$$R = \int_0^t G(u)\, du = \frac{1}{T_p}\int_{T_{om}}^{T} G(\Gamma)d\Gamma \quad (15)$$

where T_{om} is the equilibrium melting temperature. This approach remains valid as long as R is lower than the half-thickness of the sample ($e/2$).

Results

Equations (12–15) enabled us to reproduce the evolution of α and of its derivative, $d\alpha/dT$, as a function of temperature, cooling rate, and sample thickness. The data and the model generally led to calculated peaks that exhibited shoulders. The location of the peak in the scale of temperatures was generally correct. The agreement between the calculations and experiments largely depended on the thickness of the sample. For thin samples (Fig. 10), it may have seemed to be unsatisfactory, but one must keep in mind three points:

- First, peaks could not be completely recalculated because R reached its limiting value, $e/2$, during the crystallization. With the model being not valid, it was impossible to reproduce the whole peak.
- Second, V_{vol} remained very low during the crystallization, and the precision of our determination was not sufficient, especially for weak α_v's.
- Third, microscopic observations revealed that there were nearly no coarse spherulites in the 192 μm thick samples,[3] and the simple model used here was partly inaccurate for the situation where transcrystalline zones totally overlapped the sample.

So, this simple approach is not accurate for thin samples.

Agreement was most satisfactory for thicker samples (Figs. 11–13). The agreement was not always perfect, but it must be noted that the model remained simple. In addition, when making comparison between a given experiment and calculations, we compared a single value to an average evolution. Some discrepancy in such a case is not totally surprising.

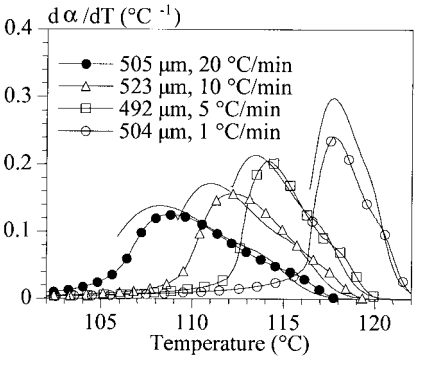

Figure 11 Comparison between (symbols) experimental DSC traces obtained with 510 μm thick samples and (—) calculations using eqs. (12–15).

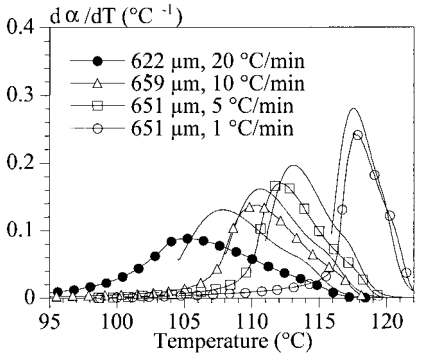

Figure 12 Comparison between (symbols) experimental DSC traces obtained with 651 μm thick samples and (—) calculations using eqs. (12–15).

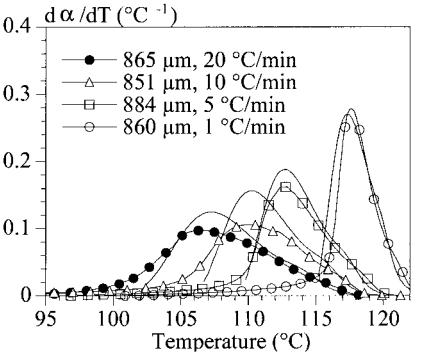

Figure 13 Comparison between (symbols) experimental DSC traces obtained with 865 μm-thick samples and (—) calculations using eqs. (12–15).

Nevertheless, it was possible to reproduce DSC traces and to correctly locate crystallization temperatures. This represents a validation for the determinations presented here.

GENERAL CONCLUSIONS

It is possible to analyse DSC experiments when important transcrystalline zones exist. Provided that transcrystalline nuclei are numerous and are nucleated in a quasi instantaneous mode, methods are available to characterize both the nucleating ability of the surface and the intrinsic crystallization of the polymer. These methods consist of the analysis of the crystallization at constant cooling rates of samples of different and calibrated thicknesses.

The thinner samples must be thin enough to ensure that their crystallization results mainly from transcrystalline zones. Then, simple manipulations give rise to the number of nuclei per unit surface that promote transcrystallinity and to an approximate value of G of the polymer as a function of temperature.

Measurements performed with at least three different thicknesses allowed us, independently from the previous estimate, to determine the crystallization kinetics of the polymer itself, that is, those not disturbed by transcrystallinity. This latter determination could then be used to obtain the crystallization temperature, Avrami exponent, and so on. The thickest sample must be thick enough to ensure that bulk crystallisation can occur. Of course, thermal gradients within the samples must be avoided; that is, the thickness must be limited. At cooling rates lower than 30°C/min, a thickness of 900 μm seems to be an upper limit which must not be overstepped.

These two parallel determinations were successfully carried out with a HDPE, and the method was validated with simple analytical models. Even if this technique is not yet very precise, it represents real improvement for DSC technique, because nowadays, DSC analysis is unusable when transcrystallinity occurs. Further developments dealing with the understanding of the appearance of this phenomenon and with proposals of efficient ways to avoid it are also of prime interest. Another possible extension of this work is the study of nucleating ability of material by the testing of sandwiches with the polymer in the midplane.

APPENDIX: CALCULATION OF THE VOLUME OF TRANSCRYSTALLINE ZONES, V_{SUR}

The formation of transcrystalline zones can be described by the appearance of N_s nuclei per unit surface on both sides of a film of thickness e. Let us assume nucleation to be instantaneous. Then, semispherulites grow from the surfaces in all available directions until they impinge on each other.

The volume of the transcrystalline regions is the summation of the volume of all these spherulites. To calculate this sum, the thickness of the film can be decomposed into thin slices of thickness dx and location x (Fig. A.1). In each of these slices, the appearance and the growth of disk-shaped entities (Fig. A.1) can model the crystallization. These entities are the intersection of the semispherulites and the fictitious slices.

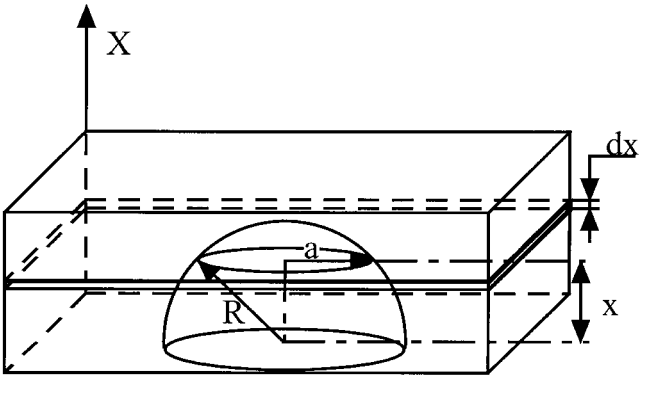

Figure A.1 Schematic model for the film.

As the nucleation is instantaneous and G is identical for all the spherulites, disk-shaped entities also exhibit an instantaneous nucleation at time t_x, depending on the location of the slice. If G is the growth rate of spherulites

$$x = \int_0^{t_x} G(u)du \tag{A.1}$$

Disk-shaped entities of a given slice grow at the same rate. At any time their radius (a) is given by (Fig. A.1):

$$a^2 = [\int_0^t G(u)du]^2 - x^2 = R^2 - x^2 \tag{A.2}$$

The surface transformed fraction in the slice (α_{sl}), can be described with the classical Kolmogoroff–Avrami–Evans theory. In that case[26]:

$$\alpha_{sl} = 1 - \exp(-N_s\pi a^2) \tag{A.3}$$

The volume of transcrystalline zones is then given by

$$V_{sur} = 2S\int_0^{e/2} \alpha_{sl}(x)dx \tag{A.4}$$

where S is the surface of the film. Finally

$$V_{sur} = 2S\left(\int_0^R (1 - \exp(-N_s\pi(R^2 - x^2)))dx\right) \tag{A.5}$$

Equation (A.5) leads easily to eq. (14) (in the main text).

If N_s and R are low, then

$$\exp[-N_s\pi(R^2 - x^2)] \approx 1 - N_s\pi(R^2 - x^2) \tag{A.6}$$

and

$$V_{sur} = 4SN_s\frac{\pi R^3}{3} \tag{A.7}$$

When R increases, V_{sur} becomes equal to $2RS$, and eq. (A.5) is consistent with the two simple models of growth of transcrystalline zones: semispherical spherulites and continuous planar fronts.[12,13]

References

1. Fraser, G. V.; Keller, A.; Odell, J. A. J Appl Polym Sci 1978, 22, 2979.
2. Kamal, M. R.; Chu, E. Polym Eng Sci 1983, 23, 27.
3. Billon, N.; Henaff, V.; Pelous, E.; Haudin, J. M. J Appl Polym Sci 2002, 86, 725.
4. Devaux, E. Ph.D. Thesis, Université "Claude Bernard" Lyon I, 1992.
5. Fitchmun, D. R.; Newman, S. J Polym Sci Part A-2: Polym Phys 1970, 8, 1545.
6. Gray, D. G. J Polym Sci Polym Lett Ed 1974, 12, 509.
7. Campbell, D.; Qayyum, M. M. J Polym Sci Polym Phys Ed 1980, 18, 83.
8. Lee, Y. C.; Porter, R. S. Polym Eng Sci 1986, 26, 633.
9. Chatterjee, A. M.; Price, F. P. J Polym Sci Polym Phys Ed 1975, 13, 2369.
10. Chatterjee, A. M.; Price, F. P. J Polym Sci Polym Phys Ed 1975, 13, 2391
11. Janeschitz-Kriegl, H. Progr Colloid Polym Sci 1992, 87, 117.
12. Billon, N.; Magnet, C.; Haudin, J. M.; Lefebvre, D. Colloid Polym Sci 1994, 272, 633.
13. Billon, N.; Haudin, J. M. J Therm Anal 1994, 42, 679.
14. Keith, H. D.; Padden, F. J., Jr. Polymer 1984, 2, 28.
15. Hoffman, J. D.; Lauritzen, J. I., Jr. J Appl Phys 1973, 44, 4340.
16. Hoffman, J. D.; Frolen, L. J.; Ross, G. S.; Lauritzen, J. I., Jr. J Res Nat Bur Stand Sect A 1975, 79, 671.
17. Hoffman, J. D. Polymer 1983, 24, 3.
18. Porcier-Denard, S. Ph.D. Thesis, Ecole des Mines de Paris, 1994.
19. Chew, S.; Griffiths, J. R.; Stachurski, Z. H. Polymer 1989, 30, 874.
20. Labaig, J. J. Ph.D. Thesis, University of Strasbourg, 1978.
21. Point, J. J.; Dosière, M. Polymer 1989, 30, 2294.
22. Ratajski, E.; Janesschitz-Kriegl, H. Colloid Polym Sci 1996, 274, 938.
23. Billon, N.; Escleine, J. M.; Haudin, J. M. Colloid Polym Sci 1989, 267, 668.
24. Billon, N. Ph.D. Thesis, Ecole des Mines de Paris, 1987.
25. Ozawa, T. Polymer 1971, 12, 150.
26. Evans, U. R. Trans Faraday Soc 1945, 41, 365.